

## Stochastic model of nonclassical light emission from a microcavity

Seiji Miyashita

*Department of Earth and Space Science, Faculty of Science, Osaka University, Toyonaka, Osaka 560, Japan*

Hiromi Ezaki

*Faculty of Engineering, Tokyo Institute of Polytechnics, Atsugi 243-02, Japan*

Eiichi Hanamura

*Department of Applied Physics, University of Tokyo, Bunkyo-ku, Tokyo 113, Japan*

(Received 1 August 1997)

A sub-Poissonian distribution of photon numbers (photon-number squeezing) within a microcavity is theoretically shown to be possible using a realistic model of nonlinear photon dissipation. By deriving and solving a stochastic Schrödinger equation for a system with photons and atoms in a microcavity, we have obtained strong antibunching and a sub-Poissonian distribution of the number of emitted photons from the microcavity. The relationship among the above three statistical quantities, which describe the nonclassical nature of the quantum radiation field, are also discussed. [S1050-2947(98)07102-9]

PACS number(s): 42.50.Lc, 42.50.Ct, 42.55.Sa

### I. INTRODUCTION

The interaction of atoms or excitons with the radiation field within microcavities has been studied extensively. The radiation field is so well quantized there that only a single mode can dominate the interaction with materials and the field amplitude increases in inverse proportion to the square root of the volume of the microcavity. Large Rabi splittings [1] and clear Rabi oscillations [2] were observed for excitons in semiconductor microcavities. A great variety of nonlinear optical responses are observed depending on the quality of the quantum wells [3–5]. The nonclassical nature has been observed for the radiation field emitted from these microcavities. For example, photon-number squeezing was observed with a semiconductor laser operating under constant current [6]. Antibunching of the luminescent light was observed from a small number of  $^{24}\text{Mg}^+$  ions under stationary pumping within a microcavity [7,8].

These phenomena have been analyzed by the Jaynes-Cummings model [9]. This model has been extended so as to include (i) cavity damping and (ii) pumping of an electronic system [10,11]. Recently, we have extended the model further to include (iii) excitonic effects, i.e., effects due to many atoms and excitation propagation. We have studied the extended model by solving an equation of motion for the reduced density matrix (RDM) [12–15] with terms representing the dissipation and the pumping effects [11].

The nonclassical features that we study here are (a) the sub-Poissonian distribution of photon numbers within a microcavity (photon-number squeezing), which is measured by the Fano factor  $\sigma^2$ , (b) the antibunching of the temporal sequence of photon emissions from the cavity, which is characterized by the second-order normalized time-correlation function  $g^{(2)}(\tau)$ , and (c) the sub-Poissonian distribution of photons emitted from the cavity. We will introduce a kind of Fano factor  $\sigma_e^2$  to measure the degree of sub- (or super-) Poissonian photon counting outside the cavity. The nonclassical features (b) and (c) are investigated by studying the

temporal sequence of photons emitted from the cavity.

So far there has been no direct investigation of the relationship between  $\sigma^2$ ,  $g^{(2)}(\tau)$ , and  $\sigma_e^2$  in a quantum-mechanical system. In the present paper, we will explore the relation among these nonclassical features by proposing concrete quantum-mechanical models.

Concerning photon-number squeezing within the cavity, we have reported that a nonclassical feature of the radiation field is possible under resonant stationary pumping of the lowest exciton [11]. The degree of sub-Poissonian distribution, however, was weak for photons within the microcavity. Namely, the Fano factor, defined by

$$\sigma^2 = \frac{\langle n^2 \rangle - \langle n \rangle^2}{\langle n \rangle}, \quad (1)$$

was as close to one as 0.94 even under optimum conditions. Here  $\text{Tr} n^2 \rho = \langle n^2 \rangle$  and  $\text{Tr} n \rho = \langle n \rangle$  are averaged with the reduced density matrix of the system  $\rho$  under the stationary condition. In the present paper, we propose a model of nonlinear photon dissipation that can realize the robust nonclassical feature of light and thus we will be able to control the degree of squeezing, i.e., the sub-Poissonian distribution of the photon-number within the microcavity. Enhancement of the photon number squeezing due to the nonlinear photon dissipation will be investigated in Sec. III.

As for the temporal characteristics, such as the antibunching of the emission and the sub-Poissonian photon counting, it is necessary to introduce a microscopic dynamical model that describes the dynamics in the stationary state. Therefore, we introduce a stochastic Schrödinger equation (SSE), i.e., a Schrödinger equation with some random modulation, to study such temporal properties of individual stochastic processes. In Sec. II this equation is derived from microscopic processes described within the density-matrix formalism. We consider that the present stochastic model can simulate the relevant behavior of realistic systems. Averaging over the stochasticity, we obtain the same result for the time evolu-

tion of quantities as is obtained by the RDM method. This SSE can be regarded as a direct realization of the method of quantum jump [16–18].

The nature of the temporal behavior of the radiation field is characterized by the second-order time-correlation function of  $I(t)$  as

$$g^{(2)}(\tau) = \frac{\langle I(t)I(t+\tau) \rangle}{\langle I(t) \rangle \langle I(t+\tau) \rangle} \quad (2)$$

where  $I(t)$  indicates the intensity of the radiation field emitted from the cavity. We obtain the trivial inequality

$$g^{(2)}(0) \geq g^{(2)}(\tau), \quad (3)$$

as long as  $I(t)$  and  $I(t+\tau)$  are considered classical variables. On the other hand, when we take into account the quantization of the radiation, we should be careful about the definition of  $g^{(2)}(0)$ . In this case,  $g^{(2)}(\tau)$  is written as [19]

$$g^{(2)}(\tau) = \frac{\langle E^-(t)E^-(t+\tau)E^+(t+\tau)E^+(t) \rangle}{\langle E^-(t)E^+(t) \rangle \langle E^-(t+\tau)E^+(t+\tau) \rangle}, \quad (4)$$

where  $\langle \rangle$  denotes the average over the distribution of  $I(t)$ . If we define

$$g^{(2)}(0) = \lim_{\tau \rightarrow 0} g^{(2)}(\tau), \quad (5)$$

then we could have

$$g^{(2)}(0) < g^{(2)}(\tau). \quad (6)$$

As has been reviewed in [20], there are two definitions of antibunching: One is given by Eq. (6) and the other is determined by the derivative of  $g^{(2)}(\tau)$  at  $\tau=0$ . When the inequality

$$g'(0) = \left. \frac{dg^{(2)}(\tau)}{d\tau} \right|_{\tau=0} > 0 \quad (7)$$

holds, the process is called antibunching; if  $g'(0) \leq 0$ , it is bunching. These definitions, however, do not always coincide. If  $g^{(2)}(\tau)$  is monotonic, both definitions coincide. For example, it has been found [21] that  $g^{(2)}(0) > 1$  and  $g^{(2)}(\tau)$  decreases monotonically for thermal radiation, which is bunching in both definitions.

The words ‘‘bunching’’ and ‘‘antibunching’’ originate from the temporal distribution of photons emitted from the system. Thus we study this distribution in Sec. IV, namely, we investigate how uniformly the radiation is distributed in time. There we study the distribution  $P_{\text{emit}}^{\delta t}(n)$  of the photon number observed outside the cavity for each time interval  $\delta t$ . We introduce a kind of Fano factor for the distribution  $\sigma_e^2(\delta t)$ , which gives another nonclassical feature of the photon emission:

$$\sigma_e^2(\delta t) = \frac{\bar{n}^2 - \bar{n}^2}{\bar{n}}, \quad (8)$$

where

$$\bar{n} = \sum_{n=0}^{\infty} n P_{\text{emit}}^{\delta t}(n), \quad \bar{n}^2 = \sum_{n=0}^{\infty} n^2 P_{\text{emit}}^{\delta t}(n). \quad (9)$$

The relation between  $\sigma_e^2$  and antibunching has been discussed [19,20,22,24]. If we assume that the probability  $p$  to count an emission in a time  $\Delta t$  is proportional to the intensity  $I$  and  $\Delta t$ , i.e.,  $p = \alpha I \Delta t$ , then the probability  $P_{\text{emit}}^{\delta t}(n)$  is given by a Poissonian distribution, where  $\alpha$  is a constant dependent on the detector. The mean of the distribution is proportional to the intensity of the radiation  $\alpha \delta t I$ . The probability  $P_{\text{emit}}^{\delta t}(n)$  should be averaged over the distribution of the intensity of the radiation. In the limit where the counting time  $\delta t$  is short compared to the coherent time over which the intensity changes,  $\bar{n}$  and  $\bar{n}^2$  are obtained as [22,23]

$$\bar{n} = \alpha \delta t \langle I \rangle$$

and

$$\bar{n}^2 - \bar{n}^2 = \alpha \delta t \langle I \rangle + (\alpha \delta t)^2 (\langle I^2 \rangle - \langle I \rangle^2).$$

In this case,  $\sigma_e^2$  is given as [19,22]

$$\sigma_e^2 = 1 + \bar{n} \frac{\langle I^2 \rangle - \langle I \rangle^2}{\langle I \rangle^2}. \quad (10)$$

Here  $\langle \rangle$  denotes an average over the distribution of  $I(t)$ . For the classical case,  $\sigma_e^2$  is always larger than 1.0. On the other hand, for quantum-mechanical systems, taking into account relation (4), the following relation is obtained [24]:

$$\begin{aligned} \sigma_e^2 &= 1 + \frac{\bar{n}}{(\delta t)^2} \int_t^{t+\delta t} dt_2 \int_t^{t+\delta t} dt_1 [g^{(2)}(t_2 - t_1) - 1] \\ &\simeq 1 + \bar{n} \left[ \lim_{\delta t \rightarrow 0} g^{(2)}(\delta t) - 1 \right]. \end{aligned} \quad (11)$$

This expression is derived when the observation time  $\delta t$  is much shorter than the time  $\tau$  characterizing  $g^{(2)}(\tau)$ . Therefore, we are careful in taking the limit  $\tau \rightarrow 0$  numerically within  $\tau > \delta t$  when we compare the stationary property  $\sigma_e^2$  and dynamical property  $g^{(2)}(\tau \rightarrow 0)$ . From this relation we can deduce the following: if  $\sigma_e^2 < 1.0$ , then the emission is antibunching, i.e.,  $\lim_{\tau \rightarrow 0} g^{(2)}(\tau) < 1$ . In Sec. IV the dependence of  $\sigma_e^2$  on  $\delta t$  and also on the degree of antibunching will be discussed.

In Sec. II we introduce the model with nonlinear photon dissipation and describe the equation of motion of the RDM and the SSE. In Sec. III strongly sub-Poissonian photon-number distributions within the microcavity are demonstrated in the model of nonlinear decay of photons. The second-order correlation function  $g^{(2)}(\tau)$  of photon emission and the temporal distribution of emissions are evaluated in Sec. IV. A possible mechanism of antibunching and sub-Poissonian photon counting is discussed from the viewpoint of the existence of dead time [20] in the present dynamical process in Sec. V. Section VI is devoted to a summary and discussion for future problems.

## II. MODEL AND METHOD

In order to study the properties of photons emitted from a microcavity, we study a generalized Jaynes-Cummings model in which a single-mode photon is coupled with a system of interacting two-level atoms:

$$\begin{aligned} \mathcal{H} = & \hbar \omega_0 \sum_j S_j^z - \hbar J \sum_j (S_j^+ S_{j+1}^- + S_j^- S_{j+1}^+) + \hbar \omega_L b^\dagger b \\ & + \hbar g \sum_j (S_j^+ b + S_j^- b^\dagger), \end{aligned} \quad (12)$$

where  $S^z$  and  $S^{+(-)}$  are spin operators with  $S=1/2$  describing the two-level atom and  $b^\dagger$  and  $b$  are the boson creation and annihilation operators of the cavity photon. Here we restrict ourselves to the resonant condition  $\omega_0 = \omega_L$  for simplicity. Throughout the present paper we use the vacuum Rabi frequency as the unit of energy, i.e., we set  $g=1.0$ .

Using the method of Markovian reduced density of state [12–14], we investigate the dynamics of the model (12) when it is coupled with incoherent processes, such as photon dissipation and pumping of the electronic system:

$$\frac{\partial \rho}{\partial t} = -\frac{i}{\hbar} [\mathcal{H}, \rho] + \Gamma_F \rho + \Gamma_A \rho. \quad (13)$$

Here we adopt the photon dissipation process  $\Gamma_F$  in the form

$$\Gamma_F \rho = -\kappa (b^\dagger b \rho - 2b \rho b^\dagger + \rho b^\dagger b) \quad (14)$$

and the pumping process [15]

$$\Gamma_A \rho = -\alpha \sum_j (S_j^- S_j^+ \rho - 2S_j^+ \rho S_j^- + \rho S_j^- S_j^+). \quad (15)$$

We calculate the time evolution of Eq. (13) by making use of the following decomposition of the time evolution operator for a time slit  $\Delta t$ :

$$e^{\Delta t(\mathcal{L} + \Gamma_F + \Gamma_A)} \rho \rightarrow e^{\Delta t \mathcal{L}} e^{\Delta t \Gamma_F} e^{\Delta t \Gamma_A} \rho,$$

where  $\mathcal{L} \rho = (i\hbar)^{-1} [\mathcal{H}, \rho]$  and  $e^{A(t)}$  denotes the time-ordered exponential of a time-dependent operator  $A(t)$ . This is the lowest approximation, but we have checked that the precision is sufficient by changing the value of the time slit  $\Delta t$  over  $\Delta t=0.001$ – $0.01$ . If desired, higher-order decompositions [25] can be used to obtain higher precision.

In the previous study [11] the dependence of  $\sigma^2$  on the pumping rate  $\alpha$  and photon decay rate  $\kappa$  were studied, where the parameter  $\kappa$  was independent of the photon density. There we found that photon-number squeezing can be realized under stationary conditions, but the degree of squeezing was limited to  $\sigma^2 \approx 0.94$ .

In the present paper we introduce a model with a nonlinear dependence of the photon dissipation on the photon density in order to control more efficiently the distribution of photon numbers within the microcavity. Namely, we adopt

$$\kappa(n) = \kappa_0 + \kappa_1 n. \quad (16)$$

There are two mechanisms of introducing nonlinear decay of photons in a microcavity. In the first case, the microcavity

including the mirrors consists of nonlinear optical materials so that the dielectric constant of the system depends on the photon number within the microcavity. Therefore, the effective transmittance of this microcavity depends on the photon number. We set the microcavity at a point of inflection of the transmission spectrum for a small number of photons and then can increase the photon decay rate in proportion to the photon number. In the second case, we use a material where two-photon absorption due to a biexciton affects the nonlinear dissipation of photons. When the energy dissipation through biexcitons is so rapid, we may eliminate adiabatically the biexciton degree of freedom and describe this effect as a nonlinear decay of photons [26]. These two channels will be discussed in detail in the Appendix. The effects of excitons, i.e., collective modes coming from the interaction among atoms, will be studied elsewhere.

In this paper we study processes described by Eq. (13) with the nonlinear relaxation rate. In the general theory of dissipation, the term  $\Gamma_F \rho$  should be given in the form

$$\Gamma_F \rho = 2V \rho V^\dagger - \rho V^\dagger V - V^\dagger V \rho \quad (17)$$

and the photon-number dependence of  $\kappa(n)$  in Eq. (16) corresponds to taking the form of  $V$  as

$$V^\dagger = \sqrt{\kappa_0 + \kappa_1 b^\dagger b} b b^\dagger. \quad (18)$$

The explicit matrix element of Eq. (17) is

$$\begin{aligned} & 2\sqrt{\kappa(n+1)}\sqrt{n+1}\rho_{n+1,m+1}\sqrt{\kappa(m+1)}\sqrt{m+1} - m\kappa(m)\rho_{nm} \\ & - \rho_{nm}n\kappa(n), \end{aligned} \quad (19)$$

where  $n, m$  are the number of photons. Here we have used relations such as

$$\langle n | b \rho b^\dagger | m \rangle = \sqrt{(n+1)(m+1)} \rho_{n+1,m+1}.$$

The photon statistics are evaluated by solving Eq. (13) for both the stationary and transient phenomena. This RDM method gives the time evolution of the probability distribution of the system. Thus we can obtain the time evolution of averaged quantities.

In order to study the time sequence of the photon emission from the microcavity, it is necessary to solve the time evolution for each process, namely, a kind of the Langevin equation for the process that includes some explicit random modulation. Here we introduce a stochastic Schrödinger equation that gives the same statistical properties of the system as those obtained by RDM formalism (13). We confine ourselves to the case with a single atom in the present paper. The state of the system at time  $t$  is given as

$$|t\rangle = c|n-1, +\rangle + d|n, -\rangle, \quad (20)$$

where  $n$  denotes the photon number and  $+$  and  $-$  denote the up (excited) and down (ground) states of the atom, respectively. If an emission of a photon from the cavity occurs, then the state jumps to

$$|t'\rangle = c'|n-2, +\rangle + d'|n-1, -\rangle. \quad (21)$$

We can determine the probability of photon emission during the time interval  $\Delta t$  and the coefficients  $c'$  and  $d'$  from Eq. (13). The state (20) is described in the density matrix as

$$\rho_n = \begin{pmatrix} cc^* & cd^* \\ dc^* & dd^* \end{pmatrix} \quad (22)$$

in the space  $(|n-1, +\rangle, |n, -\rangle)$ . The quantum-mechanical motion is given by  $e^{-iH\Delta t}|t\rangle$  and the incoherent decay process is given by Eq. (17). The density matrix (22) changes by the incoherent process to

$$\rho'_n = \begin{pmatrix} [1 - 2\Delta t \kappa(n-1)]cc^* & \{1 - \Delta t[\kappa(n) + \kappa(n-1)]\}cd^* \\ \{1 - \Delta t[\kappa(n) + \kappa(n-1)]\}dc^* & [1 - 2\Delta t \kappa(n)]dd^* \end{pmatrix}$$

is defined in the space  $(|n-1, +\rangle, |n, -\rangle)$ . This is interpreted as the process in which an initial pure state is modified into a mixed state of  $n$  photons and  $n-1$  photons, namely,

$$\rho_n \rightarrow (1-q)\rho'_n + q\rho_{n-1}, \quad (24)$$

where  $\rho_n$  is a density matrix for a pure state. From Eq. (23) we can identify the state in the space  $(|n-2, +\rangle, |n-1, -\rangle)$  to be

$$|t\rangle_{n-1} = \frac{\sqrt{\kappa(n-1)}c|n-2, +\rangle + \sqrt{\kappa(n)}d|n-1, -\rangle}{\sqrt{\kappa(n-1)|c|^2 + \kappa(n)|d|^2}} \quad (25)$$

and

$$q = 2\Delta t[\kappa(n-1)|c|^2 + \kappa(n)|d|^2]. \quad (26)$$

With probability  $1-q$ , the state remains in the original space, but the coefficients are modified as

$$|t\rangle' \propto \sqrt{1 - 2\Delta t \kappa(n-1)}c|n-1, +\rangle + \sqrt{1 - 2\Delta t \kappa(n)}d|n, -\rangle. \quad (27)$$

The choice between states (27) and (25) is made stochastically. Namely, we generate a uniform random number  $v$  in  $[0, 1]$  and compare it with  $q$ . If  $v \leq q$ , then Eq. (25) is chosen; otherwise, Eq. (27) is chosen.

For the pumping process (15), a similar procedure is adopted. Under  $\Gamma_A$  the state (22) is changed into

$$\begin{pmatrix} \begin{pmatrix} cc^* & (1-x)cd^* \\ (1-x)dc^* & (1-2x)dd^* \end{pmatrix} & 0 \\ 0 & \begin{pmatrix} 2xdd^* & 0 \\ 0 & 0 \end{pmatrix} \end{pmatrix}, \quad (28)$$

$$\Gamma_F \begin{pmatrix} 0, 0 \\ 0, \rho_n \end{pmatrix} = \begin{pmatrix} \rho'_{n-1}, & 0 \\ 0, & \rho'_n \end{pmatrix} \quad (23)$$

in the space  $(|n-2, +\rangle, |n-1, -\rangle, |n-1, +\rangle, |n, -\rangle)$ , where

$$\rho'_{n-1} = 2\Delta t \begin{pmatrix} \kappa(n-1)cc^* & \sqrt{\kappa(n)\kappa(n-1)}cd^* \\ \sqrt{\kappa(n)\kappa(n-1)}dc^* & \kappa(n)dd^* \end{pmatrix}$$

is defined in the space  $(|n-2, +\rangle, |n-1, -\rangle)$  and

within the space  $(|n-1, +\rangle, |n, -\rangle, |n, +\rangle, |n+1, -\rangle)$ . Here  $x = \alpha\Delta t$ . The system jumps to the new state  $|n, +\rangle$  with probability  $2x|d|^2$ . The wave function in the original space is identified as

$$|t\rangle' \propto c|n-1, +\rangle + (1-x)d|n, -\rangle \quad (29)$$

of  $O(\Delta t)$ . Thus we compare the random number  $v$  with  $2x|d|^2$  and choose the state (29) or  $|n, +\rangle$ .

In Fig. 1(a) a typical example of the time evolution of the expectation value of the photon number  $\langle n(t) \rangle$  is shown for the parameters  $\kappa_0 = 0.1$ ,  $\kappa_1 = 0.1$ , and  $\alpha = 0.1$ . The open circle, closed circle, and cross denote three samples of  $\langle n(t) \rangle$ . From this figure we can read the equation of motion of photons for one ensemble: The photon number  $n$  first oscillates with the Rabi frequency and second decreases or increases due to photon decay or pumping, respectively. In Fig. 1(b) the average photon number  $\langle\langle n(t) \rangle\rangle$  and the average population inversion  $\langle\langle m(t) \rangle\rangle$  over 1000 samples are shown by open squares and open circles, respectively. Here  $\langle\langle \rangle\rangle$  denotes the average of the expectation value over the stochasticity. The error bars for the average are much smaller than the size of the symbols. The solid lines denote results for  $\langle\langle n(t) \rangle\rangle$  and  $\langle\langle m(t) \rangle\rangle$  obtained by solving the equation of motion of the RDM, Eq. (13). Hereafter we express  $\langle\langle \rangle\rangle$  by  $\langle \rangle$  for simplicity. In the figure, we have confirmed that the present stochastic model gives the same time evolution as that of Eq. (13).

We also study the stationary state by the SSE. For example, we obtain  $\langle n \rangle = 0.33 \pm 0.01$  and  $\sigma^2 = 0.87 \pm 0.01$  for the parameters  $\kappa_0 = 0.1$ ,  $\kappa_1 = 0.1$ , and  $\alpha = 0.1$ . Here we estimated the error bars as the standard deviation over five bins (group of samples) of  $10^6$  samples. The corresponding data obtained by the RDM are  $\langle n \rangle = 0.33$  and  $\sigma^2 = 0.87$ . Thus we again confirm the equivalence of the two methods for averaged quantities.

The present method involving the time evolution of the wave function is a kind of Langevin equation equivalent to Eq. (13), which could be called a stochastic Schrödinger equation. This type of stochastic procedure has been termed

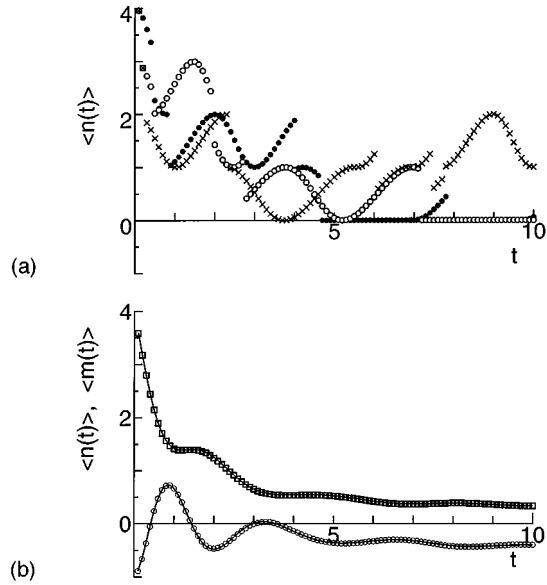


FIG. 1. (a) Samples of the time evolution of the expectation of the photon number  $\langle n(t) \rangle$  within the microcavity for  $\kappa_0=0.1$ ,  $\kappa_1=0.1$ , and  $\alpha=0.1$ . The different symbols denote different samples of the time evolution by the SSE. (b) The square denotes the ensemble average of  $\langle n(t) \rangle$  and the solid line through the squares denote  $\langle n(t) \rangle$  obtained by the RDM. The same for the population difference  $\langle m(t) \rangle$  is given by circles. The unit of time is the inverse of the Rabi frequency  $g$ , which maintains throughout the paper.

the method of quantum jump [16–18] and the present the SSE can be regarded as an example of this. The relation between SSE and the RDM is similar to that between the Langevin equation and the Fokker-Planck equation. The individual transition probability in the SSE cannot be justified from more fundamental mechanics. In this sense, the SSE is just a stochastic model that provides the same statistical property as the RDM, namely, Eq. (13). However, just like the case of the kinetic Ising model, the SSE may provide a qualitative description of the dynamics of realistic models. The kinetic Ising model has been introduced to provide the canonical ensemble of states in the steady state, but it is actually used to study the qualitative nature of the relaxational motion of uniaxial magnets [27–30]. Thus we adopt the present procedure as a first step in the study of the temporal properties of emission. This SSE is applied to evaluate antibunching and dead time effect on the photon emission from the microcavity in Secs. IV and V, respectively.

### III. PHOTON-NUMBER SQUEEZING WITHIN THE MICROCAVITY

In this section the photon statistics are evaluated by solving the time evolution of Eq. (13) and the Fano factor  $\sigma^2$  [Eq. (1)] is calculated. This shows that the degree of sub-Poissonian nature is enhanced by the nonlinearity in the decay rate of photons. This sub-Poissonian nature (photon-number squeezing) is one of the most significant nonclassical features of the radiation field within the microcavity and can be measured, e.g., by quantum nondemolition measurements. In Table I we list an example of the dependence of  $\sigma^2$  on  $\kappa_0$  and  $\kappa_1$ . When the number of photons within the microcavity  $\langle n \rangle$  is large, the nonlinearity enhances the degree of the sub-

TABLE I. Fano factor ( $\sigma^2$ ) for  $t=50$  (stationary state).

$\kappa_0$	$\kappa_1$	$\alpha$	$\langle m \rangle$	$\langle n \rangle$	$\sigma^2$
0.00	0.001	0.3	0.00	11.86	0.54
0.00	0.003	0.3	0.01	6.78	0.56
0.00	0.005	0.3	0.01	5.18	0.57
0.00	0.01	0.3	0.01	3.56	0.61
0.00	0.05	0.3	-0.01	1.41	0.73
0.00	0.10	0.3	-0.06	0.94	0.75
0.00	0.30	0.3	-0.21	0.49	0.75
0.00	0.50	0.3	-0.26	0.34	0.78
0.00	0.70	0.3	-0.27	0.26	0.81
0.00	1.00	0.3	-0.25	0.18	0.85
0.00	2.00	0.3	-0.10	0.08	0.92
0.10	0.001	0.3	-0.03	1.51	0.99
0.10	0.003	0.3	-0.04	1.45	0.97
0.10	0.005	0.3	-0.04	1.39	0.95
0.10	0.01	0.3	-0.04	1.28	0.92
0.10	0.05	0.3	-0.09	0.88	0.83
0.10	0.10	0.3	-0.14	0.69	0.80
0.10	0.30	0.3	-0.24	0.41	0.78
0.10	0.50	0.3	-0.27	0.29	0.80
0.10	0.70	0.3	-0.27	0.23	0.83
0.10	1.00	0.3	-0.24	0.16	0.86
0.10	2.00	0.3	-0.09	0.08	0.93
0.30	0.001	0.3	-0.19	0.59	0.91
0.30	0.003	0.3	-0.19	0.59	0.90
0.30	0.005	0.3	-0.19	0.58	0.90
0.30	0.01	0.3	-0.20	0.57	0.89
0.30	0.05	0.3	-0.22	0.50	0.86
0.30	0.10	0.3	-0.24	0.43	0.84
0.30	0.30	0.3	-0.28	0.30	0.82
0.30	0.50	0.3	-0.27	0.23	0.84
0.30	0.70	0.3	-0.25	0.18	0.86
0.30	1.00	0.3	-0.21	0.14	0.88
0.30	2.00	0.3	-0.06	0.07	0.94
0.50	0.001	0.3	-0.26	0.38	0.88
0.50	0.003	0.3	-0.26	0.38	0.88
0.50	0.005	0.3	-0.26	0.37	0.88
0.50	0.01	0.3	-0.26	0.37	0.88
0.50	0.05	0.3	-0.27	0.34	0.87
0.50	0.10	0.3	-0.27	0.31	0.86
0.50	0.30	0.3	-0.27	0.23	0.85
0.50	0.50	0.3	-0.26	0.18	0.86
0.50	0.70	0.3	-0.23	0.15	0.88
0.50	1.00	0.3	-0.18	0.12	0.90
0.50	2.00	0.3	-0.03	0.06	0.94
0.00	0.001	0.5	0.01	15.46	0.52
0.00	0.001	0.8	0.02	19.59	0.51
0.00	0.001	1.0	0.02	21.87	0.51

Poissonian nature as is naturally expected. It is noted that  $\sigma^2$  has a minimum point as a function of  $\kappa_1$  for nonzero  $\kappa_0$ . On the other hand,  $\sigma^2$  decreases monotonically with  $\langle n \rangle$  when  $\kappa_0=0$ .

For a very small number of photons in the microcavity,

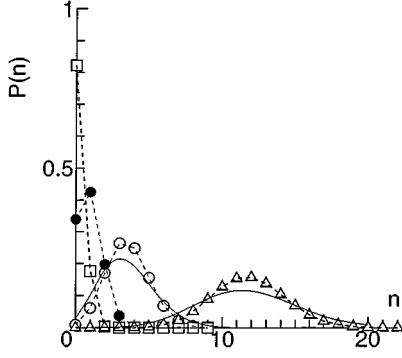


FIG. 2. Photon distribution  $P(n)$  for the parameters  $(\kappa_0, \kappa_1, \alpha) = (0.0, 0.001, 0.3)$  where  $\sigma^2=0.54$  and  $\langle n \rangle = 11.86$  ( $\triangle$ ),  $(0.0, 0.01, 0.3)$  where  $\sigma^2=0.61$  and  $\langle n \rangle = 3.56$  ( $\circ$ ),  $(0.0, 0.1, 0.3)$  where  $\sigma^2=0.75$  and  $\langle n \rangle = 0.94$  ( $\bullet$ ), and  $(0.0, 1.0, 0.3)$  where  $\sigma^2=0.85$  and  $\langle n \rangle = 0.18$  ( $\square$ ). The solid lines show the Poissonian distributions with  $\langle n \rangle = 11.86$  and  $3.56$ .

the distribution of the photon number  $P(n)$  almost localizes at  $n=0$  or  $1$ . Here  $P(n)$  is the probability that the system has  $n$  photons within the microcavity. For cases with  $n=0$  or  $1$ ,  $\langle n^2 \rangle = \langle n \rangle$  and the Fano factor is given approximately by

$$\sigma^2 = \frac{\langle n^2 \rangle - \langle n \rangle^2}{\langle n \rangle} \approx 1 - \langle n \rangle = 1 - P(1). \quad (30)$$

Thus the degree of sub-Poissonian nature seems to become weaker when the number of photons becomes smaller, i.e., when  $\kappa_1$  or  $\kappa_0$  increases. In this low-photon-density region, however, the concept of the sub-Poissonian may not have a significant meaning.

The photon-number distributions  $P(n)$  are drawn in Fig. 2 for  $\kappa_1 = 0.001, 0.01, 0.1$ , and  $1.0$ . The average photon number  $\langle n \rangle$  in the microcavity is  $11.86, 3.56, 0.94$ , and  $0.18$ , respectively. The sub-Poissonian distribution of the photon number within the microcavity is clear for cases with large  $\langle n \rangle$ , i.e.,  $\sigma^2 = 0.54$  and  $0.61$  for  $\kappa_1 = 0.001$  and  $0.01$ , respectively. For comparison, the Poissonian distributions for  $\langle n \rangle = 11.86$  and  $3.56$  are drawn by thin solid lines.

In order to study cases with larger values of  $\langle n \rangle$  we investigate the model with stronger pumping, i.e.,  $\alpha = 0.5, 0.8$ , and  $1.0$ . The Fano factor seems to converge to  $0.5$  when  $\langle n \rangle$  increases [31]. If we consider stronger nonlinearity for  $\kappa(n)$ , such as a cubic function or a step function of the photon number  $n$ , however, we could have smaller values of  $\sigma^2$ . Here we confine ourselves to the nonlinearity given by Eq. (16).

#### IV. ANTIBUNCHING EMISSION AND SUB-POISSONIAN PHOTON COUNTING

Nonclassical features of emitted photons are discussed in this section by regarding the photon decay as equivalent to photon emission. Of course, the dissipation of photons does not necessarily mean the emission of photons. Here, however, we assume that the photon dissipation comes only from the leakage of photons from the microcavity. Thus the first mechanism for the nonlinearity of the dissipation (16) is more suitable for the present assumption.

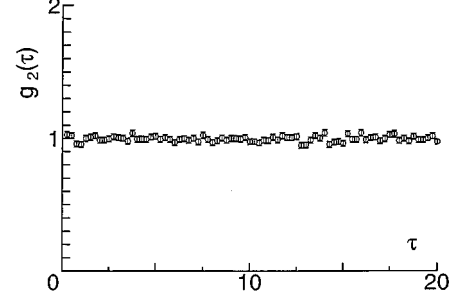


FIG. 3.  $g^{(2)}(\tau)$  for  $\kappa_0=0.0$ ,  $\kappa_1=0.01$ , and  $\alpha=0.3$ .

The ensemble-averaged photon intensity emitted from the cavity is expressed as

$$\begin{aligned} I^e(t) &= \text{Tr}\{\rho(t) V^\dagger V\} \\ &= \text{Tr}\{\rho(t) \sqrt{\kappa_0 + \kappa_1 b^\dagger b} b^\dagger b \sqrt{\kappa_0 + \kappa_1 b^\dagger b}\} \\ &= \text{Tr}\{\rho(t) (\kappa_0 + \kappa_1 b^\dagger b) b^\dagger b\}. \end{aligned} \quad (31)$$

Thus the averaged emission intensity from a state with  $n$  photons is proportional to  $\kappa(n)n$ .

##### A. Antibunching

First, the second-order correlation function  $g^{(2)}(\tau)$  is evaluated to detect the photon antibunching characteristics after the system reaches the stationary state. In the simulation with the SSE, we store the time of each emission. In order to calculate  $g^{(2)}(\tau)$ , we make a coarse graining of the emission process. That is to say we divide the time sequence into a discrete mesh and count the numbers of emissions in each interval ( $\delta t = 0.25$ ). In this way, we obtain the time sequence of emission  $\{I(j), \text{ for } j=1, \dots, j_{\max} = T/\delta t\}$ , where  $T$  is the total observation time. Then we calculate the correlation function (2) in the discrete mesh:

$$g^{(2)}(m) = \frac{1}{n_{\text{emit}}^2} \sum_{j=0}^{j_{\max}-m} \frac{I(j)I(j+m)}{j_{\max}-m}, \quad (32)$$

where  $n_{\text{emit}}$  is the average number of emissions in an interval  $\delta t$ . Because of the stationarity, we set here  $\langle I(t) \rangle = \langle I(t + \Delta t) \rangle = n_{\text{emit}}$ . We simulated five different time sequences of  $T = 2.0 \times 10^4 [2.0 \times 10^7 \Delta t (= 0.001)]$ . The error bar in the figures denotes the standard deviation over these five samples.

In the cases where a large degree of squeezing was realized studied in Sec. III antibunching is not found. For example, in Fig. 3,  $g^{(2)}(\tau)$  is shown for  $\kappa_0 = 0.0$ ,  $\kappa_1 = 0.01$ , and  $\alpha = 0.3$ . For this set of parameters,  $g^{(2)}(\tau)$  is almost flat, although strong squeezing  $\sigma^2 = 0.61$  was found. Here the average number of emission  $n_{\text{emit}}$  is  $0.074$ .

In order to realize antibunching, we reduce the photon number within the microcavity by increasing the relaxation rate. First, we take  $\kappa_0 = 0.0$ ,  $\kappa_1 = 0.1$ , and  $\alpha = 0.3$ ;  $g^{(2)}(\tau)$  is shown in Fig. 4(a), where  $n_{\text{emit}} = 0.079$ . Here we find a small dip for small  $\tau$ , which is supposed to be a sign of antibunching, but the process is still almost Poissonian.

Next, we consider cases with stronger damping, where the distribution of more than two photons within the microcavity

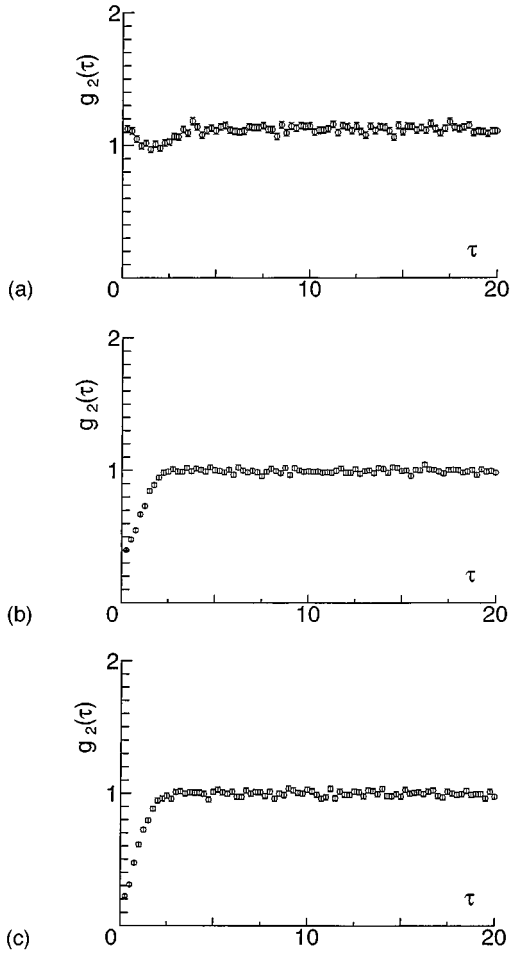


FIG. 4.  $g^{(2)}(\tau)$  for  $\alpha=0.3$  and (a)  $\kappa_0=0.0$  and  $\kappa_1=0.1$ , (b)  $\kappa_0=0.0$  and  $\kappa_1=1.0$ , and (c)  $\kappa_0=0.0$  and  $\kappa_1=2.0$ .

is almost zero, i.e.,  $P(n) \approx 0$  for  $n \geq 2$ . In Fig. 4(b),  $g^{(2)}(\tau)$  is drawn for  $\kappa_0=0.0$ ,  $\kappa_1=1.0$ , and  $\alpha=0.3$ . For this set of parameters, we find that  $g^{(2)}(\tau)$  becomes small as  $\tau$  approaches to zero. We thus conclude that the present sequence of emissions shows antibunching. Here  $n_{\text{emit}} \sim 0.094$ . If we increase the value of  $\kappa_1$ , stronger antibunching is found. In Fig. 4(c) the results for  $\kappa_1=2.0$  are also plotted, where  $n_{\text{emit}} \sim 0.082$ . The recovery time of antibunching will be discussed in Sec. V.

It should be noted that when we increase the decay rate, the number of photons within the microcavity  $\langle n \rangle$  decreases, while the number of emitted photons  $n_{\text{emit}}$  does not depend heavily on the rate.

Now we discuss the relation between  $\sigma^2$  for photons within the microcavity and antibunching of the emitted photons. The antibunching nature becomes more clear as the nonlinear decay rate  $\kappa_1$  increases. On the other hand, the degree of squeezing decreases with the increase of  $\kappa_1$ , for example, the Fano factor  $\sigma^2$  is 0.61, 0.75, 0.85, and 0.92 for  $\kappa_1=0.01, 0.1, 1.0$ , and  $2.0$ , respectively. As was mentioned in Sec. III, for a very small number of photons in the microcavity, the concept of the sub-Poissonian distribution may not have a significant meaning. The average photon numbers within the microcavity  $\langle n \rangle$  are 3.56, 0.94, 0.18, and 0.08, for  $\kappa_1=0.01, 0.1, 1.0$ , and  $2.0$ , respectively. For realization of antibunching, it seems important that the distribution  $P(n)$

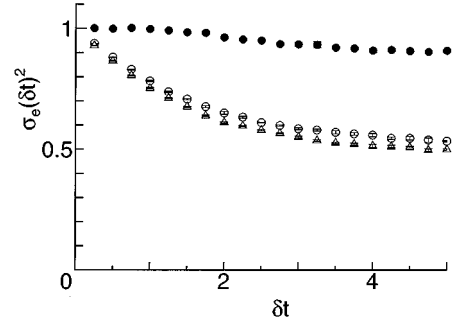


FIG. 5. Dependence of  $\sigma_e^2$  on  $\delta t$  for the cases shown in Fig. 4.  $\bullet$ ,  $\circ$ , and  $\triangle$  denote the data for  $\kappa_1=0.1, 1.0$ , and  $2.0$ , respectively.

localizes only over  $n=0$  and  $1$ , as shown by open squares in Fig. 2. Thus we cannot find the correlation between the Fano factor  $\sigma^2$  of photon number within the microcavity and the antibunching  $g^{(2)}(\tau)$  of photons emitted from the microcavity. This is in contrast to the relation of the antibunching property to the Fano factor  $\sigma_e^2$  of the distribution of photons emitted from the microcavity, which is defined in the following subsection.

### B. Sub-Poissonian photon counting

Next we obtain the distribution  $P_{\text{emit}}^{\delta t}(n)$  of the numbers of emitted photons in a time interval  $\delta t$ , which corresponds to the photon number counting outside the microcavity. Here we divide the observation time  $T$  into  $T/\delta t$  intervals and calculate  $P_{\text{emit}}^{\delta t}(n)$  by counting how many intervals contain  $n$  emitted photons. The distribution depends on  $\delta t$  and the  $\delta t$  dependence of the Fano factor  $\sigma_e^2$  is shown in Fig. 5. Here we can discuss the relation between the Fano factor  $\sigma_e^2$  and antibunching  $g^{(2)}(\tau)$ . For such a case in which antibunching is observable, when  $\delta t$  increases the Fano factor  $\sigma_e^2$  decreases, i.e., the nonclassical nature is enhanced as the observation interval  $\delta t$  increases beyond the characteristic time of  $g^{(2)}(\tau)$ . On the other hand,  $\sigma_e^2(\delta t)$  remains near 1.0 for the case of weak nonlinear damping  $\kappa_1=0.01$  in which the degree of antibunching is weak, i.e.,  $g^{(2)}(\tau) \approx 1$ . This behavior will be analyzed in more detail in Sec. V. Now let us consider the relation (11). For the smallest value of the observation time  $\delta t=0.25$ , we find that  $1 + \bar{n} [g^{(2)}(\tau=\delta t) - 1]$  is 1.0, 0.943, and 0.936 and that  $\sigma_e^2(\delta t)$  is 1.0, 0.943, and 0.929 for  $\kappa_1=0.01, 0.1$ , and  $1.0$ , respectively. Thus we find good agreement with the second line of Eq. (11).

We also investigated  $\sigma_e^2$  at the value  $\delta t$  where the average number of emissions  $\bar{n}$  is nearly 1.0. This quantity  $\sigma_e^2(1.0)$  is a kind of Fano factor for the distribution of the number of emitted photons in the time period for which one photon is emitted on average. For  $\kappa_1=0.1$ , we took  $\delta t=3.25$ , where  $\bar{n}=1.025 \pm 0.006$ , and obtained  $\sigma_e^2(3.25)=0.922 \pm 0.005$ . Similarly, we obtained the following: for  $\kappa_1=1.0$ ,  $\delta t=2.75$ ,  $\bar{n}=1.036 \pm 0.004$ , and  $\sigma_e^2(2.75)=0.599 \pm 0.002$  and for  $\kappa_1=2.0$ ,  $\delta t=3.00$ ,  $\bar{n}=0.993 \pm 0.003$ , and  $\sigma_e^2(3.00)=0.500 \pm 0.004$ . We conclude that when the degree of antibunching is stronger the distribution of emitted photons becomes more

sub-Poissonian. Namely, in the present model, the Fano factor  $\sigma_e^2(\bar{n}=1.0)$  has a strong correlation with the degree of antibunching found in  $g^{(2)}(\tau)$ . Here we found that the nonclassical nature of the emission can be clearly observable as the antibunching phenomenon at small time  $\tau$  and, on the other hand, as the sub-Poissonian distribution of emitted photons at large  $\delta t$  for which  $\bar{n} \geq 1$ .

It should be noted that it is only in such low-photon-density regions as  $\langle n \rangle \ll 1$  that both nonclassical features, that is, antibunching and sub-Poissonian photon counting, are clearly observed. The nonlinear dissipation produces efficiently the distribution over the photon numbers 1 and 0 and consequently the antibunching and the sub-Poissonian photon counting are enhanced.

### V. EFFECT OF THE DEAD TIME

In this section we consider the mechanism of the antibunching emission. As long as the emission probability per unit time is constant and independent of time, the distribution of the emitted photon number is expressed as

$$P_{\text{emit}}^{\delta t}(n) = {}_N C_n p^n (1-p)^{(N-n)}, \quad p = \langle n \rangle \delta t / N, \quad (33)$$

where a time interval  $\delta t$  is divided into  $N$  pieces  $\delta t / N$  and  $\langle n \rangle = \kappa(n)n$ . For the binomial distribution, we have  $\bar{n} = pN$  and  $\bar{n}^2 - n^2 = p(1-p)N$ . Thus

$$\sigma_e^2 = 1 - p. \quad (34)$$

If we take the limit  $N \rightarrow \infty$ ,  $\sigma_e^2$  becomes 1. Namely, the distribution (33) becomes the Poissonian distribution as long as  $p$  is independent of time.

When we consider the quantum-mechanical natures of excitation and emission, a dead time after each emission is inevitable. Consequently, it is not realistic to assume the binomial distribution of the number of emitted photons for every time interval of very small  $\delta t / N$ .

Let us consider the origin of the dead time. When a photon is emitted from an atom via spontaneous emission, namely, without the cavity, some time must elapse before the atom can be excited again. This gives rise to a dead time [7]. Furthermore, when the atom is in a cavity, there is an additional contribution to the dead time from the process that the excited atom emits a photon in the cavity.

In the microcavity, the atom interacts coherently with photons by Eq. (12) and the emission from the cavity is given by the mechanism of Eq. (14). There a state is expressed as

$$|\phi(n)\rangle = c(t)|n-1, +\rangle + d(t)|n, -\rangle. \quad (35)$$

The emission is counted when a photon exits the cavity through a wall. The probability of emission is proportional to that of the dissipation of photons:

$$p_{\text{emit}} = |c(t)|^2 \kappa(n-1)(n-1) + |d(t)|^2 \kappa(n)n. \quad (36)$$

If the dissipation is very strong compared to the pumping, only the probabilities  $P(0)$  and  $P(1)$  have significant values. In such a case the emission occurs only when  $|d(t)|^2 \neq 0$ . After the emission of a photon, the state changes to  $|0, -\rangle$ . It

then takes some time to restore  $d(t)$ , which causes the dead time. First, the atom must be excited, namely,  $|0, -\rangle \rightarrow |0, +\rangle$ . The time  $t_{01}$  to pump the atom ( $\alpha = 0.3$ ) is estimated as

$$t_{01} = \frac{1}{2\alpha} = \frac{5}{3}. \quad (37)$$

Here let us remember the unit of time to be the inverse of the Rabi frequency  $g$ . A second contribution to the dead time comes from the duration for which the atom emits a photon in the microcavity. The time  $t_{02}$  for the system to change from  $|0, +\rangle$  to  $|1, -\rangle$  is roughly given by

$$t_{02} = \frac{T_{\text{Rabi}}}{4} = \frac{2\pi}{4\omega_{\text{Rabi}}} = \frac{1}{2}\pi. \quad (38)$$

The dead time is given by the sum of these two contributions

$$t_0 = t_{01} + t_{02}. \quad (39)$$

In Figs. 4(b), 4(c), and 5 we can see that the characteristic time is about 1.0–2.0 for  $\kappa_1 = 1.0$  and 2.0, which is consistent with the  $\tau$  dependence of  $g^{(2)}(\tau)$ . This characteristic time is of the same order as the above estimate of  $t_0$ . On the other hand, the characteristic time for  $\kappa_1 = 0.1$  is much longer. This dependence is understood as follows: For  $\kappa_1 = 1.0$  and 2.0, the photon dissipates with high probability when photons appear within the microcavity for the first time. On the other hand, the photon dissipation is so weak for  $\kappa_1 = 0.1$  that the photon may not dissipate but rather excite the atom again. Namely, the process  $|1, -\rangle$  to  $|0, +\rangle$  takes place. Then the system has to wait until the next time region for which  $|d(t)|^2 \sim 1$ . Under this situation, the higher photon number states are produced through such pumping process as  $|n, -\rangle$  to  $|n, +\rangle$ , so that the effect of dead time is smeared out.

Now let us consider the effect of the dead time  $t_0$  on the emission of photons. During the dead time, the emission of a photon is suppressed. Thus it naturally causes antibunching, i.e., the reduction of  $g^{(2)}(\tau)$ . We can study the effect of dead time on the photon-counting statistics by looking at the distribution  $P_{\text{emit}}^{\delta t}(n)$ . If we consider a constant probability  $\kappa(n)n$  of photon emission, the distribution of emitted photons during an interval  $\delta t$  is the Poissonian distribution, as was pointed out above. If we take into account the dead time, however, the time available for the photon emission from the cavity is reduced by  $t_0$  per every emission. Generally, the distribution  $P_{\text{emit}}^{\delta t}(n)$ , with the dead time taken into account, has a complicated form. Here let us confine ourselves to the case  $\delta t \geq t_0$  for simplicity, where the overlap of dead times can be neglected. Then the probability of  $k$  emissions  $P_{\text{emit}}^{\delta t}(k)$  has to be modified as

$$P_{\text{emit}}^{\delta t}(k) = ({}_{N-Mk} C_k) p^k (1-p)^{(N-Mk-k)}, \quad M = t_0 N / \delta t. \quad (40)$$

If we take the limit  $N \rightarrow \infty$  keeping  $M/N = t_0 / \delta t$  to constant,  $P_{\text{emit}}^{\delta t}(k)$  is rewritten as

$$P_{\text{emit}}^{\delta t}(k) = \frac{1}{k!} [\langle n \rangle \delta t (1-rk)]^k \exp[-\langle n \rangle \delta t (1-rk)], \quad (41)$$

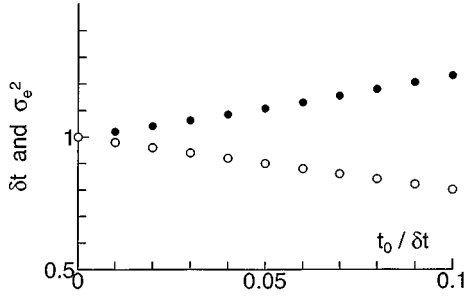


FIG. 6. ● and ○ denote  $\delta t$  and  $\sigma_e^2$ , respectively.  $\Delta t$  is normalized by the value for  $t_0=0$ .

where  $r = t_0 / \delta t$ . This modified Poissonian distribution shows a sub-Poissonian nature, i.e.,  $\sigma_e^2 < 1.0$ . In Fig. 6 the  $\sigma_e^2$  is drawn as a function of  $t_0 / \delta t$  as open circles, keeping the average number of emitted photons to 1. The length of the interval  $\delta t$  is also shown as closed circles.

Thus we conclude that the antibunching and the degree of sub-Poissonian nature of the distribution of the emitted photon number are strongly related to the existence of the dead time after an emission. We find that the antibunching emission occurs only when  $\langle n \rangle$  is very small. This is understood as follows: When the distribution  $P(n)$  at large  $n$  is not small, more than two values of  $n$  contribute to the emission and the effect of the dead time at each  $n$  is smeared out. Thus the degree of antibunching is very much reduced. The small  $\langle n \rangle$  means that the quantum number of the system  $n$  is 1 or 0, where large fluctuation of  $n$  is suppressed and the antibunching is clearly observable.

## VI. SUMMARY AND DISCUSSION

In this paper we have studied the nonclassical features of photon emission, making use of direct numerical analyses of a quantum-mechanical system. In particular, introducing a nonlinear decay mechanism, we have observed a strong sub-Poissonian distribution of the photon number within the microcavity. So far, photon-number squeezing has been realized only in semiconductor lasers operating under constant current injection [6]. This may be called externally controlled photon-number squeezing. On the other hand, in the present paper we have presented a large amount of intrinsic photon-number squeezing under the presence of nonlinear dissipation.

We have proposed an alternative formalism, the stochastic Schrödinger equation, and solved to obtain the degree of antibunching  $g^{(2)}(\tau)$  and the sub-Poissonian degree  $\sigma_e^2$  of a photon emitted from the cavity. It has been found that the antibunching and sub-Poissonian distribution originate from the existence of the dead time after a photon emission. In the present study we have found the antibunching of the emitted light only for a small number of photons within the microcavity, while squeezing is visible for a large number of photons.

It should be noted that the present results may strongly relate to the dynamical model that we adopted. There is no microscopic justification of the stochastic treatment for the stochastic Schrödinger equation. The present model should be considered as one of possible ways in which the Jaynes-

Cummings model can be coupled to external degrees of freedom. In the present paper photon dissipation has been treated as equivalent to emission from the microcavity. In this sense, the first mechanism discussed in Sec. I and the Appendix is relevant to the present study. When the second mechanism, photon dissipation through electronic excitation and its subsequent relaxation into the reservoir, is operative, we must include an additional term representing this effect in  $\Gamma_{FP}$  of Eq. (14). The number of atoms was restricted to one in the present paper. The case of many atoms interacting with each other is a problem for the future. We hope the present paper gives a starting point for further developments.

## ACKNOWLEDGMENTS

The authors would like to thank Professor K. M. Slevin for his kind critical reading of this manuscript. This work was supported by the Grant-in-Aid from the Ministry of Education. Some of the calculations were done in the supercomputer center at the ISSP of University of Tokyo. The use of this facility is very much appreciated. H.E. would also like to thank the Hayashi Memorial Foundation for Female Natural Science and Esso Research Grants for Women for their financial support.

## APPENDIX: MECHANISM OF THE NONLINEAR DISSIPATION

Let us discuss the feasibility of the methods of generating the nonclassical light described in Sec. II. First we will discuss the first mechanism making use of a Fabry-Pérot cavity containing nonlinear optical materials. The transmission rate  $T(\omega)$  for the Fabry-Pérot cavity is sensitive to the photon number within the microcavity. The transmission rate  $T(\omega)$  is given as

$$T(\omega) = \frac{1}{1 + Q \sin^2(k)}, \quad (\text{A1})$$

where  $Q$  is the  $Q$  value of the cavity  $Q = 4R/(1-R)^2$ . Here  $R$  is the reflection rate of the walls and  $k = n_0 \omega L / c + (n_2 \omega L / c) N$ , where the refractive index of the walls is given by  $n(N) = n_0 + n_2 N$ , with  $N$  being the number of photons within the microcavity and  $L$  the width of the wall.

The decay rate  $2\kappa(N)$  from the Fabry-Pérot cavity is given by

$$2\kappa = \frac{c}{n(N)L} (1-R) = \frac{c}{n(N)L} T(\omega). \quad (\text{A2})$$

Here let us consider the Fabry-Pérot cavity under the optimum condition, namely,

$$\frac{n_0 \omega L}{c} = -\frac{\pi}{4}, \quad (\text{A3})$$

and set

$$\frac{n_2 \omega L}{c} N \equiv \frac{\delta}{2}. \quad (\text{A4})$$

Expanding  $2\kappa$  of Eq. (A2) in  $\delta$ ,

$$2\kappa \approx \frac{c}{n(N)L} \left[ \frac{1}{1+Q/2} + \left( \frac{1}{1+Q/2} \right)^2 Q \frac{n_2 \omega L}{c} N \right]$$

$$= 2\kappa_0 \left( 1 + \frac{Q}{1+Q/2} \frac{n_2 \omega L}{c} N \right), \quad (\text{A5})$$

where

$$2\kappa_0 = \frac{c}{n(N)L} \frac{1}{1+Q/2}, \quad (\text{A6})$$

then the nonlinear decay rate,  $\kappa_1 N$  is given by  $\kappa_0 n_2 \omega L Q N / c (1 + Q/2)$ . Making the relation with Eq. (A3), we have

$$\frac{\kappa_1}{\kappa_0} = \frac{\pi}{4} \frac{Q}{1+Q/2} \frac{n_2}{n_0}. \quad (\text{A7})$$

Therefore, in order to have the same order of nonlinear and linear decay,  $n_2$  should be the same order as  $n_0$ . In a microcavity, this condition should be possible.

Here it should be noted that in order to realize a very rapid change of  $\kappa(n)$  for a few photons, the required nonlinearity is the same order of magnitude as for the quantum computer, i.e.,  $n_2 N \omega L / c \sim \pi/2$ . We will be able to reduce the linear decay rate  $\kappa_0$  by using a microcavity with extremely large  $Q$  values.

The other channel of nonlinear decay is brought about by two-photon absorption due to a biexciton and  $2\kappa_1$  is estimated to be  $10^{13}$ /sec for two photon resonant absorption by a biexciton within the microcavity with volume  $\lambda^3$ . This becomes larger than  $2\kappa_0$  for a realizable system. Thus the present mechanism can provide a strong nonlinear decay rate [32].

- 
- [1] C. Weisbuch, M. Nishioka, A. Ishikawa, and Y. Arakawa, *Phys. Rev. Lett.* **69**, 3314 (1992).
- [2] T. B. Norris, J.-K. Rhee, C.-Y. Sung, Y. Arakawa, M. Nishioka, and C. Weisbuch, *Phys. Rev. B* **50**, 14 663 (1994).
- [3] T. R. Nelson, Jr., E. K. Lindmark, D. V. Wick, K. Tai, G. Khitrava, and H. M. Gibbs, in *Microcavities and Photonic Bandgaps: Physics and Applications*, edited by J. Rarity and C. Weisbuch (Kluwer, Dordrecht, 1996), p. 43.
- [4] Y. Yamamoto, J. M. Jacobson, S. Pau, H. Cao, and G. Björk, in *Microcavities and Photonic Bandgaps: Physics and Applications* (Ref. [3]), p. 457.
- [5] E. Hanamura and T. B. Norris, *Phys. Rev. B* **54**, R2292 (1996).
- [6] S. Machida, Y. Yamamoto, and Y. Itaya, *Phys. Rev. Lett.* **58**, 1000 (1987).
- [7] F. Diedrich and H. Walther, *Phys. Rev. Lett.* **58**, 203 (1987).
- [8] Th. Basche, W. E. Moerner, M. Orrit, and H. Talon, *Phys. Rev. Lett.* **69**, 1516 (1992).
- [9] E. T. Jaynes and F. W. Cummings, *Proc. IEEE* **51**, 89 (1963).
- [10] P. Filipowicz, J. Javanainen, and P. Meystre, *Phys. Rev. A* **34**, 3077 (1986).
- [11] H. Ezaki, S. Miyashita, and E. Hanamura, *Phys. Lett. A* **203**, 403 (1995).
- [12] W. H. Louisell, *Quantum Statistical Properties of Radiation* (Wiley, New York, 1973).
- [13] R. Kubo, M. Toda, and N. Hashitsume, *Statistical Physics II* (Springer-Verlag, Heidelberg, 1991).
- [14] W. Weidlich and F. Haake, *Z. Phys.* **185**, 30 (1965).
- [15] H. Haken, in *Laser Theory*, edited by S. Flügge, *Encyclopedia of Physics Vol. XXV/2C* (Springer-Verlag, Berlin, 1970).
- [16] J. Dalibard, Y. Castin, and K. Molmer, *Phys. Rev. Lett.* **68**, 550 (1992).
- [17] K. Molmer, Y. Castin, and J. Dalibard, *J. Opt. Soc. Am. B* **10**, 524 (1993).
- [18] B. M. Garraway and P. L. Knight, *Phys. Rev. A* **49**, 1266 (1994).
- [19] X. T. Zou and L. Mandel, *Phys. Rev. A* **41**, 475 (1990).
- [20] M. C. Teich and B. E. A. Salah, in *Progress in Optics XXVI*, edited by E. Wolf (Elsevier, Amsterdam, 1988), p. 1.
- [21] E. Jakeman and E. R. Pike, *J. Phys. A* **136**, 316 (1968).
- [22] D. F. Walls and G. J. Milburn, *Quantum Optics* (Springer-Verlag, Berlin, 1995), Chap. 3.
- [23] L. Mandel, *Phys. Rev. Lett.* **49**, 136 (1982).
- [24] E. Hanamura, H. Ezaki, J. Inoue, F. Yura, and A. Itoh, in *Novel Optical Materials and Applications*, edited by I. C. Khoo, F. Simoni, and C. Umeton (Wiley, New York, 1977), p. 77.
- [25] M. Suzuki, *J. Phys. Soc. Jpn.* **61**, 3015 (1992).
- [26] H. Ezaki, G. S. Agarwal, and E. Hanamura, *Opt. Commun.* **138**, 65 (1997).
- [27] K. Kawasaki, in *Phase Transition and Critical Phenomena*, edited by C. Domb and M. S. Green (Academic, London, 1972), Vol. 2, p. 443.
- [28] S. Miyashita and H. Takano, *Prog. Theor. Phys.* **73**, 1122 (1985).
- [29] H. Tomita and S. Miyashita, *Phys. Rev. B* **46**, 8886 (1992).
- [30] P. A. Rikvold, H. Tomita, S. Miyashita, and S. W. Sides, *Phys. Rev. E* **49**, 5080 (1994).
- [31] D. F. Walls and G. J. Milburn, *Quantum Optics* (Springer-Verlag, Berlin, 1995), Chap. 7.
- [32] M. Ueda, H. Kanzaki, K. Kobayashi, Y. Toyozawa, and E. Hanamura, *Excitonic Processes in Solids* (Springer-Verlag, Berlin, 1986), Chaps. 2 and 3.